# Supporting Information

# Highly dispersed Pt nanoparticles supported on carbon nanotubes produced by atomic layer deposition for hydrogen generation from hydrolysis of ammonia borane

**Jiankang Zhang,[a,b] Chaoqiu Chen,[a,*] Shuai Chen,[a] Qingmin Hu,[a] Zhe Gao,[a] Yunqin Li,[a,b] Yong Qin[a,*]**

[a] State Key Laboratory of Coal Conversion, Institute of Coal Chemistry, Chinese Academy of Sciences, Taiyuan 030001, P. R. China

[b] University of Chinese Academy of Sciences, Beijing 100039, P. R. China

*Corresponding authors. +86 351 4040081.
E-mail addresses: chenchaoqiu@iccas.ac.cn and qinyong@sxicc.ac.cn.

1. Calculation Methods of initial TOF and linear Rate

The calculation methods used in this work were taken from Ref. 7 and 18. For the conversion of reaction ($x_c$), initial TOF and linear Rate, there are the following equations:

$$x_c = \frac{P_{atm}V_{H2}/RT}{3n_{AB}}$$

$$TOF = \frac{P_{atm}V_{H2}/RT}{n_{metal}t}$$

$$Linear - Rate = \frac{V_{H2}}{t}$$

where $P_{atm}$ is the atmospheric pressure, $V_{H2}$ is the generated gas volume, R is the universal gas constant, T is room temperature (298 K), and $n_{metal}$ is the mole number of the metallic Pt metal, and t is the reaction time when $x_c$ reaches about 35%; Initial rate of $H_2$ evolution, linear Rate, equals the rate of $H_2$ generation when $x_c$ reaches 35%, t is the reaction time when $x_c$ reaches about 35%.

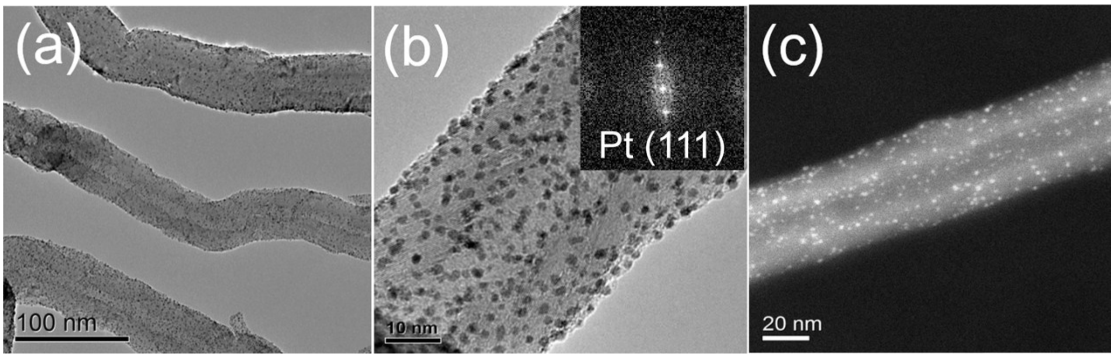


**Fig. S1** Low (a), high magnification (b) TEM images and representative (c) HAADF-STEM image of Pt20/CNTs catalysts. Insets in (b) is the FFT of single Pt nanoparticle for Pt20/CNTs catalysts.

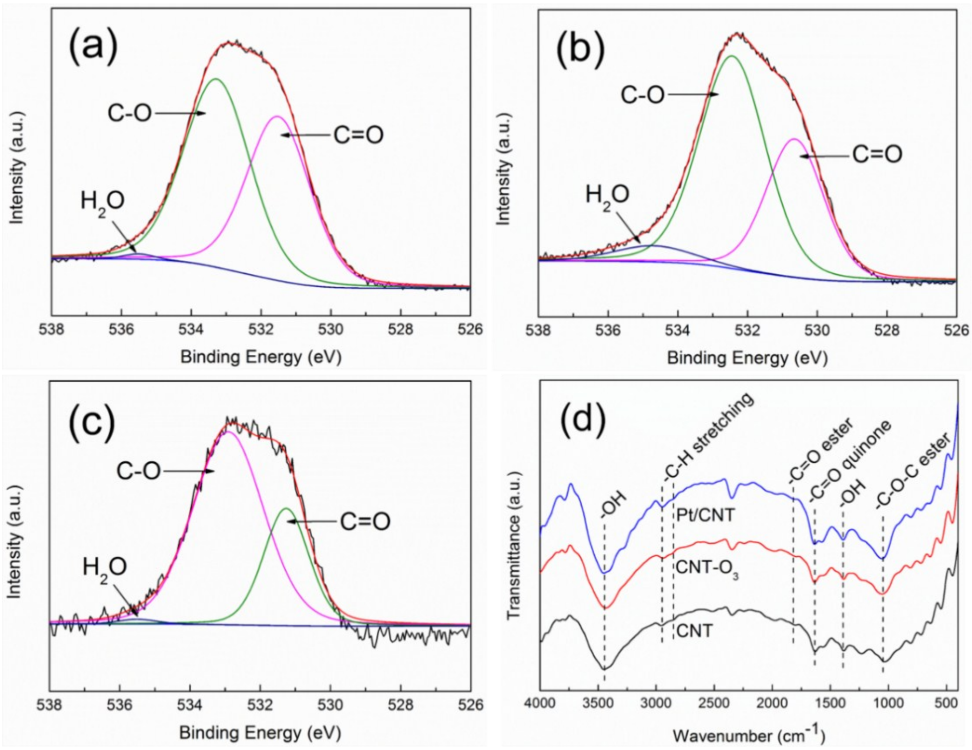


**Fig. S2** High-resolution XPS O1s of (a) CNTs, (b) $O_3$ pretreated CNTs (CNTs-$O_3$) and (c) Pt20/CNTs samples. (d) FTIR spectra of CNTs, CNTs-$O_3$ and Pt20/CNTs samples.

**Table S1** Data comparison of XPS O1s deconvolution of the different samples.

| Sample | Relative content (%) | | |
|---|---|---|---|
| | C=O | C-O | Adsorbed water |
| CNTs | 45.1 | 54.2 | 0.7 |
| CNTS-$O_3$ | 34.3 | 60.3 | 5.4 |
| Pt20/CNTs | 27.8 | 71.3 | 0.9 |

Both XPS O1s and FTIR confirm the existence of the oxygen-containing groups on CNT surface, as shown in Fig. S2a-d. The difference of oxygen-containing functional groups is not very obvious, and this is probably because that the pulse time (1 s) and exposure time (10 s) of $O_3$ to substrate (CNTs) is too short for Pt20/CNTs catalysts with 20 Pt ALD cycles.

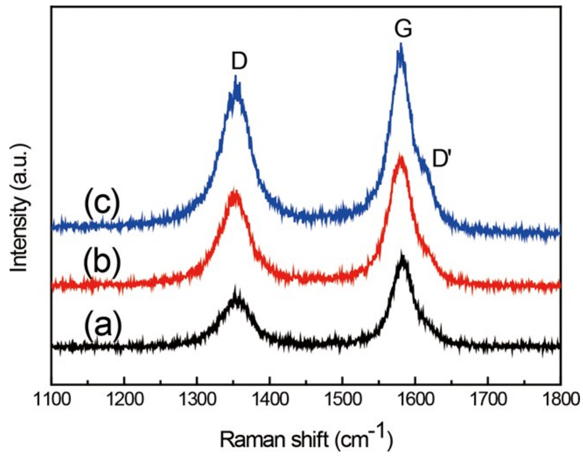


**Fig. S3** Raman spectra of (a) CNTs, (b) CNTs-$O_3$ and (c) Pt20/CNTs.

Generally, D band centered around 1352 cm$^{-1}$ and G band centered around 1579 cm$^{-1}$ in Raman spectra stand for disorder and graphite, which correspond to defect and graphite properties of CNTs. The D band is disorder induced features caused by lattice defect and is usually attributed to the presence of amorphous or disordered carbon in CNTs. While the G band reflects well-graphitized carbons in CNTs. The calculated $I_D/I_G$ value is about 0.88, 0.95 and 1.07 respectively for CNTs, CNTs-$O_3$ (pretreated with $O_3$ without pulse of MeCpPtMe$_3$) and Pt/CNTs samples. These results further confirm the existence of the oxygen-containing groups on CNT surface during the whole ALD process, which can act as active/anchoring sites for the MeCpPtMe$_3$ chemisorption, Pt nucleation and growth and finally results in a uniform dispersion of Pt nanoparticles on CNTs.

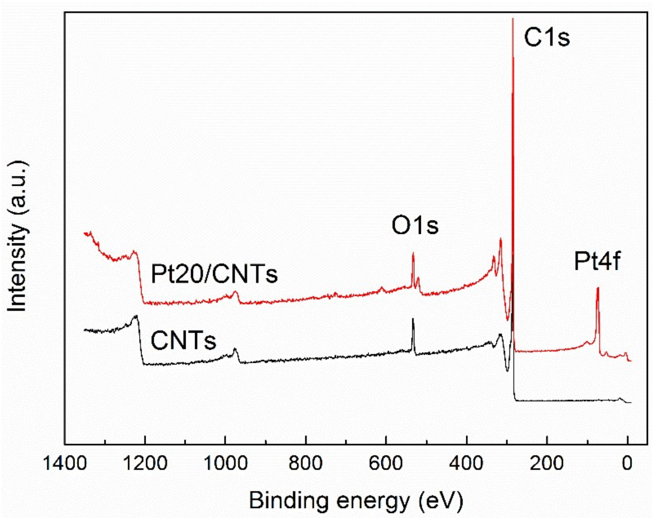


**Fig. S4** XPS survey spectra of CNTs and Pt20/CNTs samples.

**Table S2** Summary of XPS results for the Pt/CNTs catalysts with different Pt ALD cycle numbers.

| Catalysts | Relative content (%) | B.E. (eV) | Assignment | ΔBE (eV)[a] |
|---|---|---|---|---|
| | 41.3 | 71.8 | Metallic $Pt^0$ | |
| Pt10/CNTs | 44.4 | 72.8 | $Pt^{2+}$ | 0 |
| | 14.3 | 74.6 | $Pt^{4+}$ | |
| | 39.8 | 71.5 | Metallic $Pt^0$ | |
| Pt20/CNTs | 39.5 | 72.4 | $Pt^{2+}$ | 0.3 |
| | 20.7 | 74.1 | $Pt^{4+}$ | |
| | 40.5 | 71.4 | Metallic $Pt^0$ | |
| Pt40/CNTs | 40.8 | 72.2 | $Pt^{2+}$ | 0.6 |
| | 18.7 | 74.0 | $Pt^{4+}$ | |

[a] The difference of the binding energy (ΔBE) is calculated based the Pt10/CNTs catalysts.

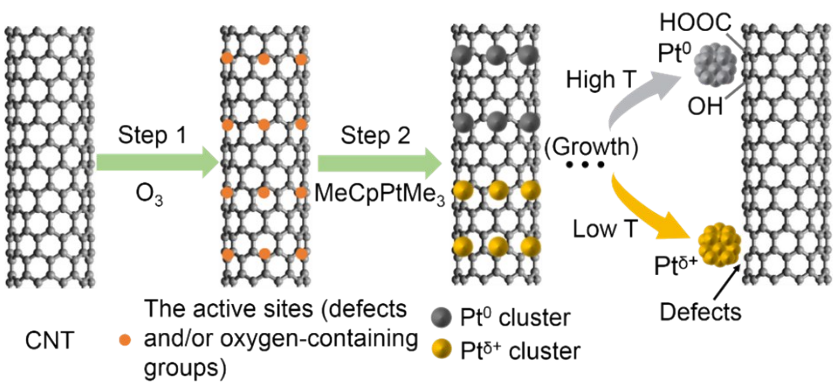


**Fig. S5** Possible ALD growth mechanism of Pt nanoparticles on CNTs.

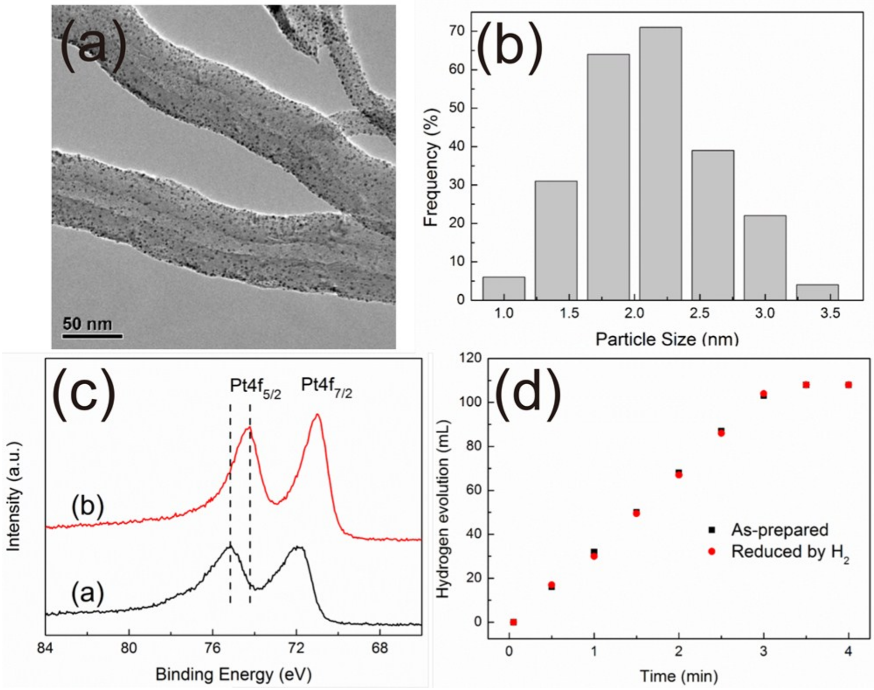


**Fig. S6.** (a) TEM image and (b) the corresponding particle size distribution of Pt20/CNTs catalysts reduced by $H_2$ at 200 $^oC$. (c) XPS spectra of Pt4f in Pt20/CNTs catalysts before (a) and after (b) $H_2$ reduction at 200 $^oC$. (d) The catalytic activity comparison of Pt20/CNTs catalysts before and after $H_2$ reduction.

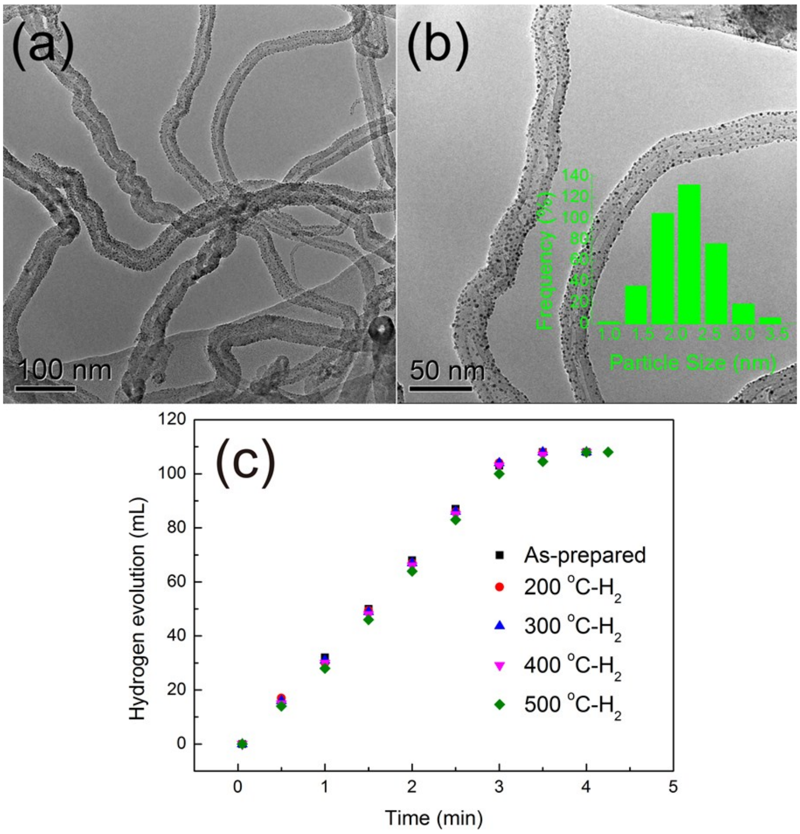


**Fig. S7** Low (a) and high (b) magnification TEM images of Pt20/CNTs catalysts reduced by $H_2$ at 400 $^{o}C$ (Inset in Fig. S7b: the corresponding particle size distribution of Pt nanoparticles). (c) Hydrogen generation from AB solution (0.15 mol/L, 10.0 mL) at 25 ± 0.5 $^{o}C$ catalyzed by the Pt20/CNTs catalysts reduced under different temperatures.

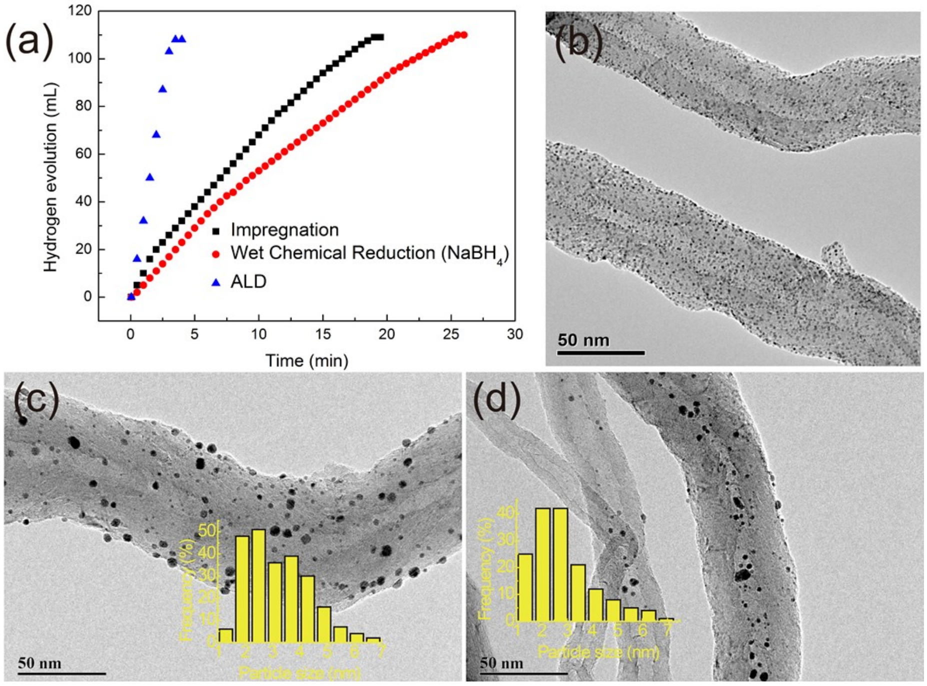


**Fig. S8** (a) Catalytic activity comparison of Pt/CNTs catalysts prepared by ALD, impregnation and wet chemical reduction, and TEM images of Pt/CNTs catalysts prepared by (b) ALD, (c) impregnation and (d) wet chemical reduction (inset in Fig S8c and S8d: the corresponding Pt nanoparticle size distribution).

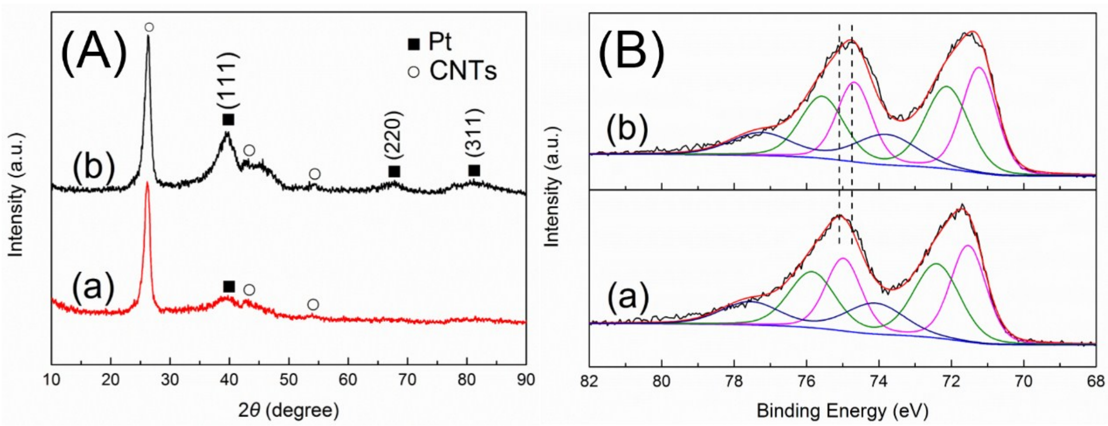


**Fig. S9** (A) XRD patterns and (B) XPS Pt4f levels of the (a) fresh and (b) deactivated Pt20/CNTs catalysts.

**Table S3** Relative content of Pt species content of the fresh and deactivated Pt20/CNTs catalysts.

| Catalysts | Relative content (%) | B.E. (eV) | Assignment | ΔBE (eV)[a] |
|---|---|---|---|---|
| | 39.8 | 71.5 | Metallic Pt | |
| Fresh | 39.5 | 72.4 | $Pt^{2+}$ | 0 |
| | 20.7 | 74.1 | $Pt^{4+}$ | |
| | 40.3 | 71.3 | Metallic Pt | |
| Deactivated | 39.3 | 72.2 | $Pt^{2+}$ | 0.3 |
| | 20.4 | 73.7 | $Pt^{4+}$ | |

[a] The difference of the binding energy (ΔBE) is calculated based the fresh Pt20/CNTs catalysts.

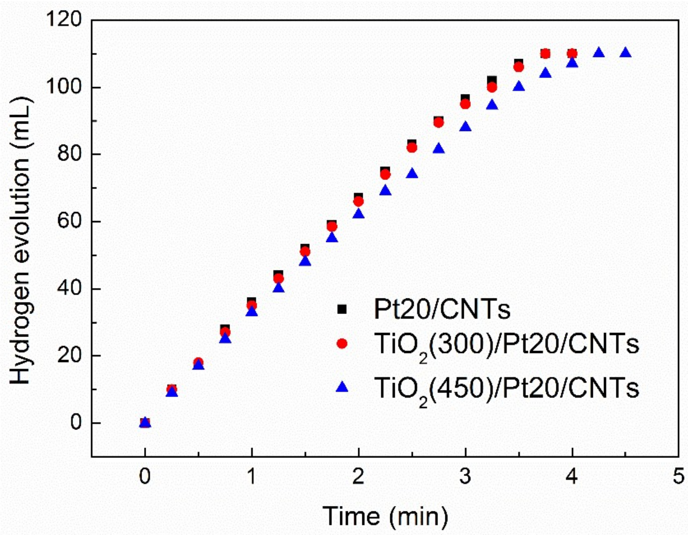


**Fig. S10** Hydrogen generation from AB solution (0.15 mol/L, 10.0 mL) catalyzed by Pt20/CNTs and calcinated $TiO_2$(300)/Pt20/CNTs and $TiO_2$(450)/Pt20/CNTs catalysts at 25 ± 0.5 °C.

**Table S4** Specific surface area and total pore volume of the as-prepared and calcinated $TiO_2$/Pt20/CNTs samples.

| Sample | $S_{BET}$ ($m^2/g$) | $V_t$ ($cm^3/g$) |
|---|---|---|
| As-prepared | 59.1 | 0.064 |
| Calcinated | 72.2 | 0.142 |

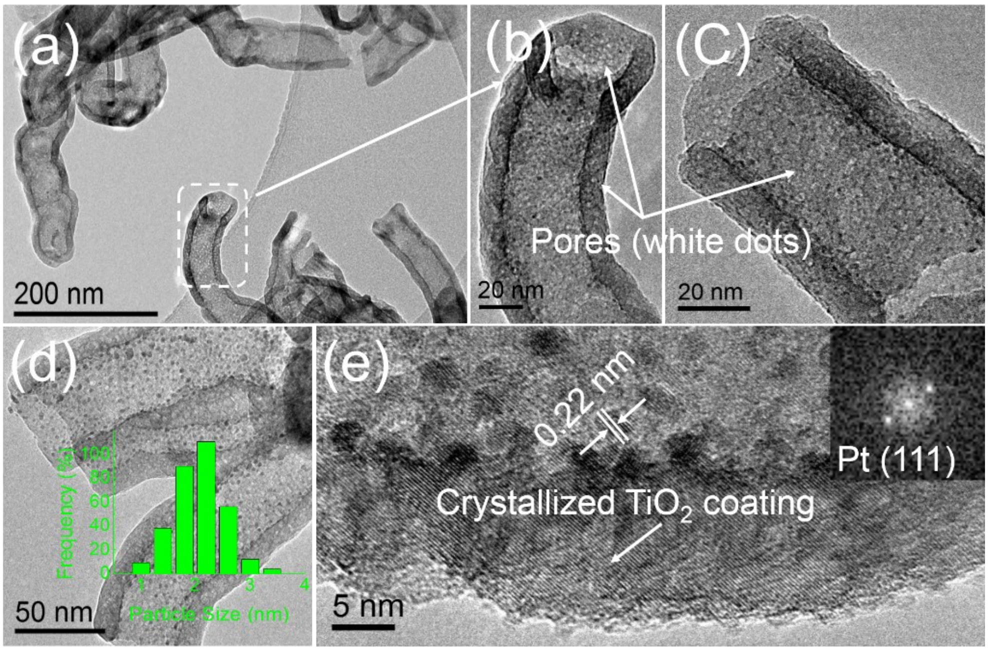


**Fig. S11** Low (a) and high magnification (b, c and d) TEM images of calcinated $TiO_2$/Pt20/CNTs catalysts. (e) HRTEM images of calcinated $TiO_2$/Pt20/CNTs catalysts. (Inset in Fig. S11d and e: the corresponding particle size distribution of the catalysts and FFT of the Pt nanoparticle; The ALD number cycle of $TiO_2$ is 300).

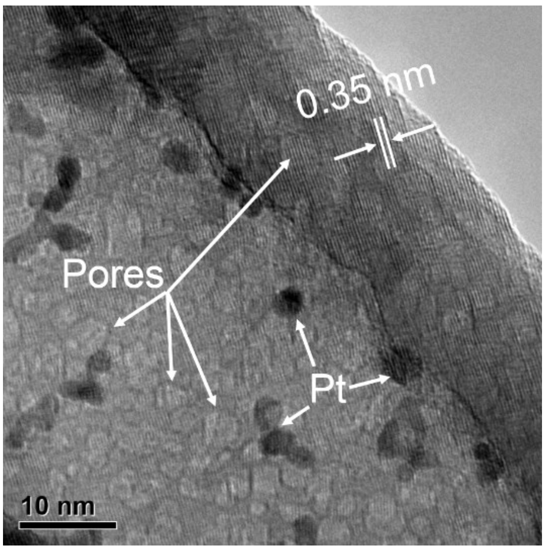


**Fig. S12** HRTEM image after ten catalytic cycles of calcinated $TiO_2$/Pt20/CNTs catalysts (The ALD number cycle of $TiO_2$ is 300).